A paraszimpatikus szabályozás hatása a duktális folyadéktermelésre egér könnymirigyben

The role of parasympathetic regulation in the fluid secretion of lacrimal gland ducts in mice

Orsolya Berczeli
Ph.D. Thesis
Doctoral School of Clinical Medicine
Supervisor: Edit Tóth-Molnár, M.D., Ph.D.
Department of Ophthalmology
University of Szeged, Szeged, Hungary

2020

TABLE OF CONTENTS

LIST OF RELATED FULL PAPERS

The thesis is based on the following publications:

1. Novel Insight Into the Role of CFTR in Lacrimal Gland Duct Function in Mice.
   INVESTIGATIVE OPHTHALMOLOGY AND VISUAL SCIENCE 2018; 59(1):54-62. (2018)

   Berczeli O, Vizvari E, Katona M, Torok D, Szalay L, Rarosi F, Nemeth I, Rakonczay Z, Hegyi P, Ding C, Tóth-Monár E.

   IF: 3.388

2. Characterization of Na^+-K^+-$2Cl^-$ Cotransporter Activity in Rabbit Lacrimal Gland Duct Cells.
   INVESTIGATIVE OPHTHALMOLOGY AND VISUAL SCIENCE 2016; 57(8): 3828-3835.
   Vizvari E, Katona M, Orvos P, **Berczeli O**, Facsko A, Rarosi F, Venglovecz V, Rakonczay Z Jr, Hegyi P, Ding C, Tóth-Molnár E.

   IF: 3.303

LIST OF ABBREVIATIONS

ANOVA	analysis of variance
BCECF-AM	2.7-bis-(2-carboxyethyl)-5-(and-6-)carboxyfluorescein-acetoxymethyl ester
BSA	bovine serum albumin
cAMP	cyclic adenosine monophosphate
$[Ca^{2+}]_i$	intracellular Ca^{2+} concentration
CF	cystic fibrosis
CFTR	cystic fibrosis transmembrane conductance regulator
DMEM	Dulbecco modified Eagle medium
FCS	fetal calf serum
FURA2-AM	Fura-2-acetoxymethyl ester
GPCR	G-protein coupled receptor
H&E	haematoxilin & eosin staining
HEPES	4-(2-hydroxyethyl)-1-piperazineethanesulfonic acid
KO	knockout
LG	lacrimal gland
PEG	polyethylene glycol
PFA	paraformaldehyde
PKA	protein kinase A
PKC	protein kinase C
ROI	region of interest
RT-PCR	real-time reverse transcription polymerase chain reaction
SEM	standard error of the mean
TBS	tris-buffered saline
VIP	vasoactive intestinal peptide
VPAC	vasoactive intestinal peptide receptor
WT	wild type

1. INTRODUCTION

1.1. Physiology of preocular tear film

The ocular surface including the cornea and conjunctiva and its overlying tear film is the first barrier of the eye to interact with the external environment. The human tear film coats the anterior surface of the eye, and is composed of three distinct layers: an inner mucin coating, a middle aqueous component, and a lipid overlay. It plays role in the inhibition of ocular surface invasion by pathogens, provides the air-tissue interface for gas exchange, and supplies essential nutrients and metabolites to maintain the integrity of the cornea. The complex tear film is secreted by the lacrimal functional unit which is composed of the ocular surface tissues, the main and accessory LGs, conjunctival goblet cells, the Meibomian glands and their interconnecting sensory and autonomic innervation. Dysfunction of these structures results in the loss of tear film homeostasis required in ocular surface maintenance and health. The lack of appropriate tear production may result in dry eye and the potential for significant surface pathology [1, 2].

The outermost portion the tear film is the lipid layer, which is secreted by the Meibomian glands, Zeiss and Moll glands. This layer contains low and high polarity of lipids and prevents evaporation and overflow of the tear fluid. The main contributor of the mid, aqueous layer is the LG, but corneal and conjunctival epithelial cells also contribute in its production. This layer constitutes the bulk of the tear film, consists of inorganic salts, glucose, urea, enzymes, proteins, glycoproteins, electrolytes, and water, provides oxygen to the corneal epithelium, washes away debris and foreign particles and contains antibacterial lysozyme. The innermost layer of the tear film is the mucous layer, which consists of membrane associated and secreted mucins, electrolytes, and water. The mucin component is produced mainly but not exclusively by the conjunctival goblet cells, but small amount of solubile mucins are secreted by the LG. The mucin layer lubricates the ocular and palpebral surface and serves to protect the cornea and conjunctiva against the abrasive effects during the blink [3, 4].

1.2. Physiology of lacrimal gland

LG contributes to the production of tear with several components. This process is mediated by an array of ion transporters/channels. More detailed understanding of the

physiology and pathophysiology of LG can lead us to find potencial pharmacological targets of dry eye disease.

LG is a tubuloacinar exocrine gland similar to other exocrine glands of the body such as the mammary gland, salivary gland and pancreas. The gland is composed of lobules separated by loose connective tissue. Such as other exocrine tubuloacinar glands, LG is composed mainly of three types of cells: acinar, ductal and myoepithelial cells. Acinar cell is the predominant cell type giving approximately 80% of all cells in the gland. These cells form the secretory unit of the gland termed as acinus. Duct cells make up to 15% of all cells in LG forming the duct system and modify the secretory product as it moves through the ducts. Similarly to acinar cells, duct cells are joined by tight junctions creating polarized cells that contribute to the unidirectional secretion of LG fluid. Myoepithelial cells are basket-shaped cells that surround the acinar cells and help to forward secreta in the ductal tree.

LG is innervated by both myelinated and unmyelinated fibers arising from the trigeminal nerve, the facial nerve, and from the superior cervical ganglion. Sympathetic nerves travel with the lacrimal artery along with parasympathetics in the zygomatic nerve. The efferent pathway originates with parasympathetic fibers from the superior salivary nucleus of the pons, which exit the brain stem with the facial nerve [1].

LG is innervated by both the parasympathetic and sympathetic nerves. The parasympathetic system predominates both anatomically and functionally. The major neurotransmitters that regulate secretion are the parasympathetic neurotransmitters acetylcholine and VIP. Anticholinergic drugs (for example tolterodine, atropine, oxybutyrin, tiotropium, and hyoscine butylbromide) or drugs with anticholinergic side effects, such as tricyclic antidepressants and antihistamines, are known to cause dry eye in humans, serving as indirect evidence for the dominant cholinergic stimulation of the LG. [5] In addition to the cholinergic agonist acetylcholine that activates M3 muscarinic receptors, parasympathetic nerves release VIP as an important regulator of tear production in humans. [6]. Sympathetic nerves release norepinephrine that can activate α- and β-adrenergic signaling pathways.

1.3. Role of LG ducts in lacrimal secretion

Acinar cell functions are widely studied, resulting in broad spectrum of information, however much less is known about the possible secretory function of duct cells. Although acini are the determining structures of tear production, the secretory role of ducts beside their piping function was also suspected for a long while. In 1972, Alexander and coworkers were

among the first pioneers who proposed the potential role of duct system in LG secretion. By using micropuncture and catheterization technique they suspected that the final fluid that reaches the ocular surface has a much higher K^+ and Cl^- composition compared to the primary fluids. They suggested that LG duct system plays an important role by modifying the compositions of the primary LG acinar fluids [7]. These data appeared to suggest that tears are formed in two distinct stages: the plasma-like primary fluid formed by acinar cells is modified by duct cells during its transit in the duct lumen.

Modifications of K^+ and Cl^- content of primary acinar fluid by ductal secretory processes were also proposed in 1981. Dartt and colleagues found high Na^+/K^+ ATP-ase density in LG duct cells by using auto-radiographic method. Electron microscopy could detect secretory vesicles in the duct cells, suggesting the notion that their role is not limited to ion and water -, but also in protein secretion [8]. However, the role of LG duct epithelium on fluid, electrolyte, and protein secretion was not well understood at that time.

Two new methods have been published to study LG duct epithelium during the past decade. Ubels and colleagues introduced the laser capture microdissection technique in LG research to perform gene expression studies on collected duct cells from frozen rat LG sections [9]. The first experimental model for the investigation of lacrimal duct function was adapted and applied by our group. Preparation of isolated intact LG ducts enabled the performance of real-time functional experiments on LG ducts for the first time. Role and regulation of various ion transporters in lacrimal duct can be studied with the use of these isolated, short-term cultured duct segments [10]. With the use of isolated duct segments, we started to investigate LG duct functions in the last few years. By a video-microscopic technique adapted and used for the first time in lacrimal duct research we investigate fluid secretion of isolated LG duct segments [11]. This technique was originally developed by Fernandez-Salazar and colleagues for the measurement of fluid secretion of pancreatic ducts [12]. Our previous experimental results gave evidence of the active role of the duct LG system in lacrimal fluid secretion.

Although earlier reports demonstrated the contribution of VIP released by parasympathetic nerves in acinar protein secretion, its impact on the fluid secretion of the LG ducts remained unknown. VIP has been discovered as a smooth-muscle-relaxant, vasodilator peptide in the lung [13], but it is also an important regulator of tear production in humans. This was illustrated by a case report of a patient who had a VIP secreting metastatic pancreatic adenocarcinoma. With an eightyfold elevated serum VIP level, this individual had an increased tear volume and decreased tear osmolarity compared to age-matched controls,

indicating that VIP increases tear production in humans, most likely by stimulating LG fluid secretion [6]. VIP binds to class II seven transmembrane spanning domain GPCR as VPAC1 and VPAC2 on the basolateral membrane of epithelial cells [14]. The VIP receptor interaction activates the G protein $G_s\alpha$ that stimulates adenylyl cyclase, that increases intracellular cAMP level. CAMP in turn activates PKA that stimulates secretion by phosphorylating target proteins. Hodges and coworkers suggested that most, but not all of VIP-stimulated protein secretion is cAMP dependent. Using a myristoylated PKA peptide inhibitor (PKI) based on the pseudosubstrate of PKA, VIP stimulated protein secretion was shown to be inhibited by about 70% [15].

Hormones and neurotransmitters, such as VIP, which raise cellular cAMP level, can stimulate acute CFTR channel activity. Our findings - based on indirect evidences - strongly suggested the role of CFTR in ductal fluid secretion as forskolin - a well-known activator of CFTR via the elevation of cytosolic cAMP levels – resulted in a significant swelling response in our experimental setup. CFTR has been shown to play a critical role in exocrine glands, such as pancreas, salivary, sweat glands and airways epithelium [16-21]. Furthermore, there are several clinical data about dry eye disease with various severity seen in CF patients, which implies the potential influence of CFTR in altered tear secretion [22-24]. Accumulating evidences from gene expression studies performed on rat and rabbit LGs demonstrated the predominant expression of CFTR in LG duct cells [9, 25, 26]. The main role of the CFTR is a regulated anion conductance in the apical membrane of many different epithelial cell types. Regulation of channel activity is predominantly via cAMP/PKA signaling [27]. The PKA-dependent phosphorylation of the CFTR protein being required for channel activity [28]. Availability of transgenic mouse models carrying genetic defects in CFTR allows us the direct examination of its role in LG [29-31].

2. AIMS OF THE STUDY

LG is the major source of tears that bathe the ocular surface and its secretion is dominantly mediated by the neurotransmitters released by the parasympathetic nerves, like acetylcholine and VIP. Although earlier reports demonstrated the presence of cholinergic and VIP receptors on LG cells and also their contribution in acinar protein secretion, the impact of parasympathetic transmitters on the fluid secretion of LG ducts is completely unknown. Therefore we aimed to investigate the role of parasympathetic stimulation induced by cholinomimetic compound carbachol or VIP on LG duct function in mouse.

CFTR plays a critical role in the transmembrane transport of chloride in many secretory epithelia. There are accumulating evidences that VIP stimulation and CFTR functions are tightly related and regulated. Therefore investigation of the role of CFTR in the parasympathetic secretory machinery in mouse LG ducts was also aimed.

Our specific aims were:

- To explore the role of cholinergic stimulation on fluid secretion in LG ducts isolated from WT and CFTR KO mice.
- To investigate fluid secretion of isolated LG duct segments evoked by VIP in WT and CFTR KO LG ducts.
- To investigate the Ca^{2+} homeostasis underlying carbachol and VIP stimulation both in WT and CFTR KO LG ducts.

3. MATERIALS AND METHODS

3.1. Animals

CFTR KO mice used throughout our studies were originally generated by Ratcliff et al. and was provided as a gift from Ursula Seidler (Hannover Medical School, Hannover, Germany) [30, 31]. The mice were congenic on the FVB/N background. A hypoxanthine phosphoribosil transferase insertion introduces a termination codon in frame with the *cftr* coding sequence to terminate prematurely the CFTR protein. No functional CFTR protein is expressed by the CFTR KO mice. Genotyping was performed by RT-PCR. The animals were kept at a constant room temperature of 24°C with a 12 h light–dark cycle and were allowed free access to specific fiber-free CFTR chow (C1013, Altromin, Lage, Germany) and drinking solution containing PEG (23 g/l PEG 4000) and high HCO^{3-} (in mM: 40 Na_2SO_4, 75 $NaHCO_3$, 10 NaCl, 10 KCl). The mice were kept in the Animal Facility of the First Department of Medicine, University of Szeged. All mice were genotyped prior to the experiments. WT refers to the +/+ littermates of the CFTR KO mice. The mice used in this study were 8-24 weeks old and weigh of 14-24 g (depending on the genotype and age). Gender ratio was 1:1 for all groups. Animals were narcotized intraperitoneally with ketamine (80 mg/kg) and xylazine (10 mg/kg) and euthanized with pentobarbital overdose (100 mg/kg).

All experiments were conducted in compliance with the ARVO Statement for the Use of Animals in Ophthalmic and Vision Research. The protocol has been approved by the Ethical Committee for the Protection of Animals in Research of the University of Szeged, Szeged, Hungary and conformed to the Directive 2010/63/EU of the European Parliament.

3.2. Solutions and chemicals

DMEM supplemented with 100 U/ml collagenase (Worthington Lakewood, NJ, USA) and 1 mg/ml bovine serum albumin was used as isolation solution. Storage solution contained DMEM and 3% (wt/vol) bovine serum albumin. Culture solution contained McCoy's 5A tissue culture medium, 10% (vol/vol) fetal calf serum, and 2 mM glutamine. Media supplements (DMEM, McCoy, FCS, glutamine and BSA) were purchased from Sigma-Aldrich (Budapest, Hungary).

Carbachol (carbamoylcholine chloride) and VIP were purchased from Sigma-Aldrich (Budapest, Hungary). Composition of solutions used in our studies is summarized in Table 1.

All chemicals listed in Table 1 were purchased form Sigma-Aldrich (Budapest, Hungary). The pH of standard HEPES-buffered solution was set to 7.4 with HCl at 37 °C. The standard HCO_3^-/CO_2 buffered solution was gassed with 95% O_2/5% CO_2 at 37 °C. FURA2-AM was purchased from Invitrogen (Waltham, MA, USA).

Compound	Content of Solutions				
	HEPES buffered solution	**HCO_3^-/CO_2^- buffered solution**	**Isolation solution**	**Storage solution**	**Culture solution**
NaCl (mM)	140	115			
KCl (mM)	5	5			
Na-HEPES (mM)	10				
$MgCl_2$ (mM)	1	1			
$CaCl_2$ (mM)	2	1			
D-Glucose (mM)	10	10			
$NaHCO_3$ (mM)		25			
Dulbecco Modified Eagle Medium			X	X	
Collagenase (U/ml)			100		
Bovine serum albumin (mg/ml)			1	0,03	
McCoy's 5A Tissue Culture Medium					X
Fetal calf serum, (vol/vol %)					10
Glutamine (mM)					2

Table 1: Composition of solutions

3.3. H&E staining

Freshly dissected LG tissues from both WT and KO mice were fixed in 4% buffered formaldehyde and embedded in paraffin. Then 3.5 μm thick serial sections were cut and stained with H&E.

3.4. Immunofluorescence

Fifteen μm thick cryostat sections were rehydrated by washing in TBS (20 mM Tris-HCl pH: 7.5, 150 mM NaCl) for 5 min, then fixed in 2% PFA. After washing the sections in TBS three times for 5 min each, the samples were permeabilized with 0,1% Triton-X in TBS for 10 to 15 min. The sections were blocked with 5% FCS in TBS for 1 hour at room temperature followed by an overnight incubation with primary antibodies for CFTR (1:100, Alomone Labs, Jerusalem, Israel), for VPAC1 (1:1000) or VPAC2 (1:250, Abcam, Cambridge, UK). Next day the samples were incubated with secondary antibody, Alexa-488 conjugated goat anti-rabbit (1:1000, Abcam, Cambridge, UK) for 1 hour and Hoechst (1:1000, Sigma-Aldrich) for 20 minutes at room temperature. The samples were examined under a Zeiss LSM 880 confocal laser scanning microscope (Oberkochen, Germany). Images were analyzed with ImageJ (NIH).

3.5. Isolation and culture of lacrimal duct segments

Mouse LG interlobular ducts were isolated as previously described by our laboratory [10]. Briefly, LGs were dissected and transferred to a sterile small flat-bottom glass flask containing a cold (4 °C) storage solution. Isolation solution was injected into the interstitium of the glands and the tissue pieces were transferred to a glass flask containing 2 ml of isolation solution. Following a 25 min incubation period in a shaking water bath at 37 °C, isolation solution was removed and 5 ml of fresh cold storage (4 °C) solution was added to the flask. LG tissue samples were transferred to a glass microscope slide and viewed under stereo microscope. Following microdissection of interlobular and intralobular LG ducts, intact LG ducts were transferred to the culture solution in a Petri dish. Isolated ducts were cultured overnight in a 37 °C incubator gassed with 5 % CO_2.

3.6. Measurement of ductal fluid secretion

Videomicroscopic technique was used for the measurement of duct fluid secretion. The method was originally developed for the measurement of pancreatic duct fluid secretion and was modified by our laboratory for the investigation of LG duct secretion [11, 12]. Fluid secretion of LG ducts was analyzed using the swelling method. Ends of isolated LG ducts seal

after overnight culture, forming a closed luminal space. Secretory process of the duct epithelium results in swelling of the ducts as the luminal space fills with the secreted fluid. The change in volume of duct lumen can be analyzed using video-microscopy.

Cultured LG duct segments were carefully transferred to a coverslip pre-treated with Poli-l-lysine. The coverslip formed the base of a perfusion chamber mounted on an inverted microscope (Olympus Ltd., Budapest, Hungary). The chamber was perfused with solutions via an infusion pump at approximately 2.5 ml/min. The temperature of perfusion chamber was maintained at 37 °C. Ducts were visualized at high magnification (40 x objective). Bright-field images were acquired at set time intervals (1 min in case of ductal fluid secretion experiments) using a charge-coupled device camera connected to a PC. Both the duration of experiments and the time intervals between images were defined in Xcellence software. An image series in TIFF-format was generated containing all of the collected data from the same experiment. Scion Image (Scion Corporation, Frederick, MD, USA) software was used to analyze changes to obtain values from the area corresponding to the luminal space in each image. The initial lumen length (L_0) and the lumen area (A_0) were measured directly from the pixel intensities on the first image. The lumen diameter was calculated assuming cylindrical setup of the duct, from the formula $2R=A_0/L_0$. The luminal surface area was calculated as $2\pi R_0 L_0$, also assuming cylindrical geometry. Measurements from subsequent individual images were normalized to the first lumen area in the series (A_0) thus giving values for the relative area ($AR=A/A_0$). Relative luminal volume ($VR=V/V_0$) of the ducts was then calculated from the relative image area. These calculations were done using Scion Image and Microsoft Excel software.

In fluid secretion measurements the investigated compounds were added to the perfusate after 10 min of superfusion with HEPES-buffered or HCO_3^-/CO_2-buffered solution. Perfusion was changed to hypotonic solution for 5 min at the end of each experiment in order to confirm epithelial integrity. Complete sealing was proved by rapid swelling as a response to hypotonic challenge. Data obtained from ducts not showing swelling response were discarded.

3.7. Measurement of $[Ca^{2+}]_i$

$[Ca^{2+}]_i$ was measured using Ca^{2+}-sensitive fluorescent dye FURA 2AM (4–5 μM) as described earlier [10]. Changes in $[Ca^{2+}]_i$ were measured using an imaging system (Xcellence; Olympus, Budapest, Hungary). Four to 5 small areas (ROIs) of 5 to 10 cells were excited in

each intact duct with light at 340 and 380 nm, and the 380/340 fluorescence emission ratio was measured at 510 nm. Results are expressed as maximum value of the 380/340 fluorescence emission ratio [F_{max} ($_{380/340}$)]. One [Ca^{2+}]$_i$ measurement was obtained per second.

3.8. Statistics

Kruskal-Wallis test with Dunn method was used for the analysis of tear secretion. A mixed ANOVA model was applied for the calculation of ductal fluid secretion. Effects of the stimulatory compounds (VIP or carbachol) were taken into account as ″fixed effects″. The effect of the individual ″duct″ and the ″duct and effects of VIP or carbachol″ interaction (we assumed that the value of the effect of the stimulatory compounds depend on the individual duct) were taken into account as random effects in the model. Statistical software (SigmaPlot Systat; Software, Inc., London, UK) was used to analyze the data, which were presented as means ± SEM. A value of $P < 0.05$ was regarded as significant.

4. RESULTS

4.1. H&E staining of LGs from WT and CFTR KO mice

The morphologic differences between LGs originated from KO and WT mice were investigated by H&E staining. Freshly dissected LGs of 8 – 10 and 20 – 24 week-old animals were processed. No obvious structural changes have been observed in KO LG tissues as compared to their age-matched WT counterparts. Figure 1 shows demonstrative images of H&E staining of LG from WT and KO mice.

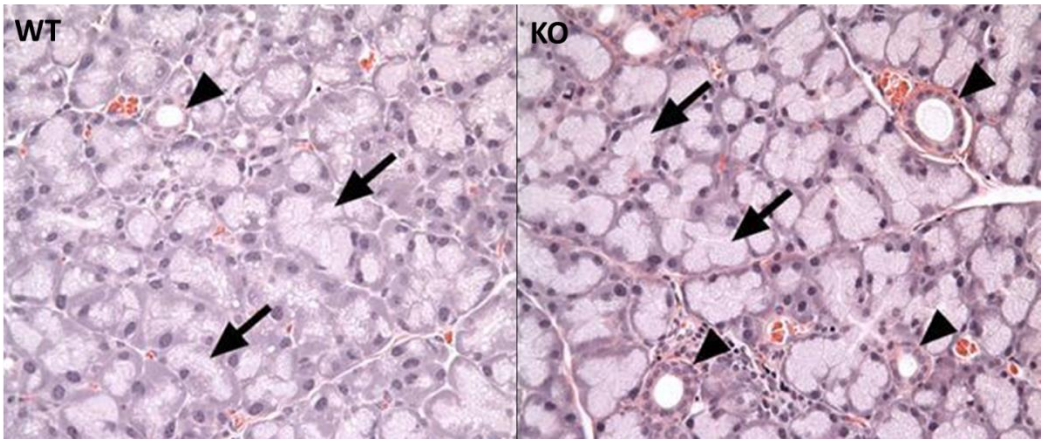

Figure 1: H&E staining of LG tissues from WT and CFTR KO mice. There are no significant morphologic changes of the KO LGs, including ducts (arrowheads) and acinar cells (arrows) compared to WT tissues.

4.2. Immunofluorescence

Immunofluorescence was used to confirm the presence of VPAC1, VPAC2 receptors and CFTR in mouse LG duct cells. We proved the presence of CFTR protein most prominently in the apical membranes of LG duct cells from WT animals, although some diffuse staining was also found in acinar cells, mostly within the cytoplasm. As anticipated, we were unable to detect the presence of CFTR protein in LGs originated from KO mice (Figure 2).

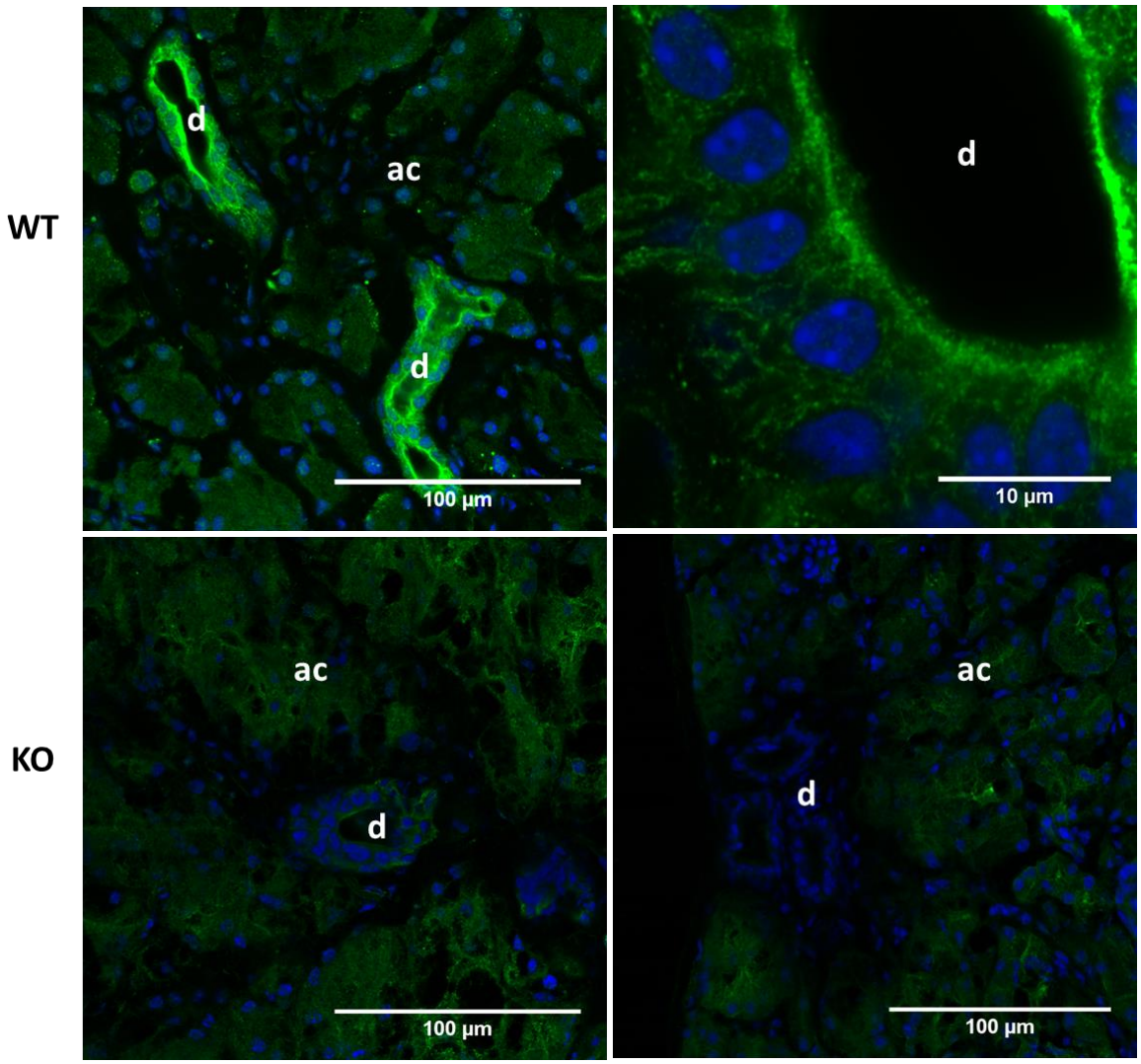

Figure 2: Immunofluorescence staining of CFTR in LG tissues from WT and CFTR KO mice. CFTR staining was most intense in the apical membranes of duct cells (d), compared to acinar cells (ac). No staining could be observed in LGs from KO mice. Hoechst was used to stain nuclei as blue.

VPAC1 is dominant in the duct cells as demonstrated in Figure 3. Immunofluorescence staining of VPAC1 receptors revealed a mosaic pattern in the expression of the receptor proteins. Intensity of fluorescence varied excessively in the investigated duct segments from the intense immunofluorescence to the lack of staining. No difference was detected in the immunoreactivity between LG tissues of WT and KO mice.

Intense VPAC2 staining was detected not only in the duct cells but also in the basolateral surface of the acinar cells (Figure 3). Intensity of immunofluorescence staining was similar in case of both WT and KO mice.

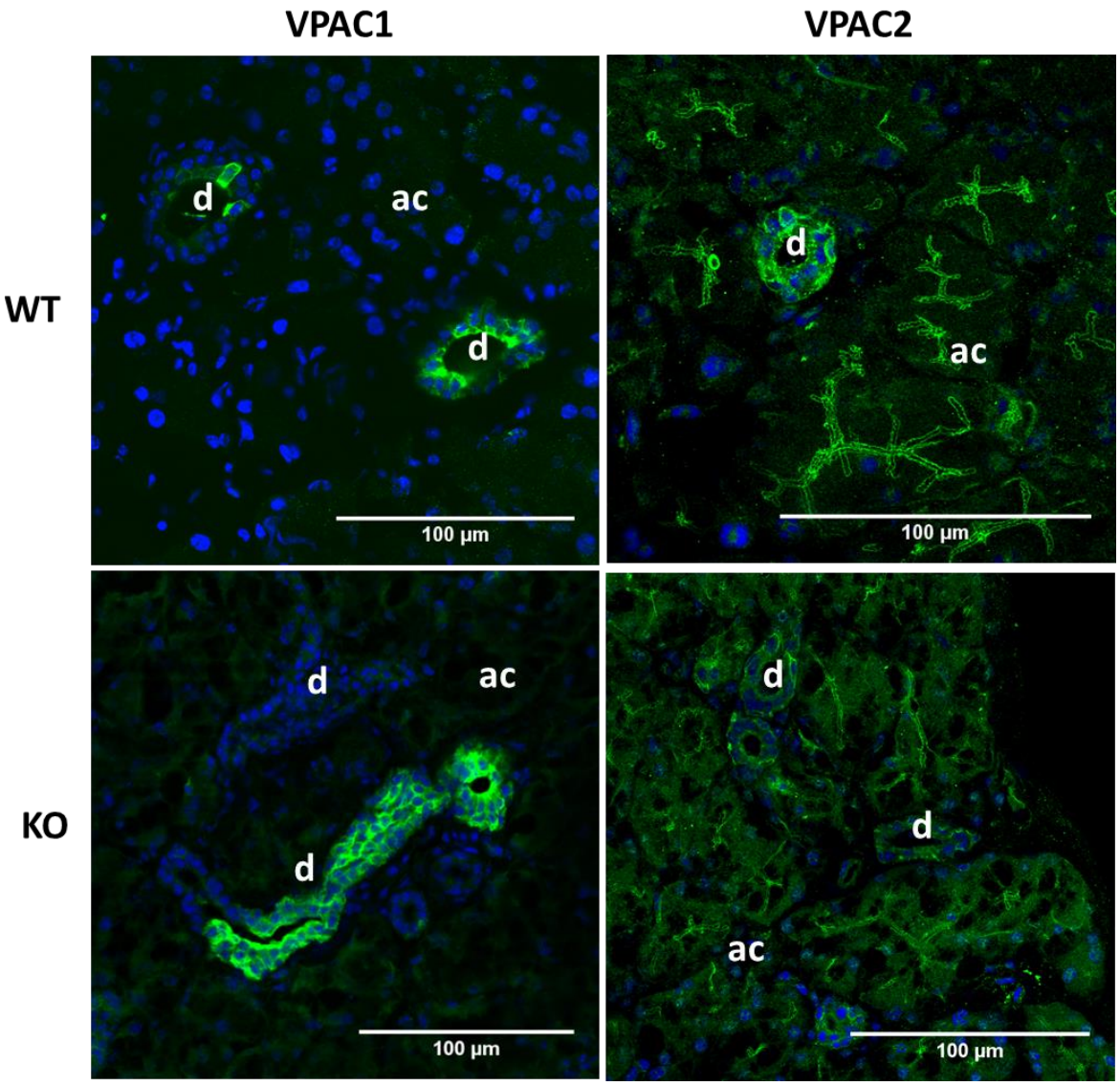

Figure 3: Immunofluorescence staining of VPAC1 and VPAC2 receptors in LGs of WT and KO mice. VPAC1 staining was more intense in ducts (d) than acinar (ac) cells. We observed VPAC2 in the basolateral surface of both duct (d) and acinar (ac) cells. There were no significant differences between WT and KO samples in case of both VPAC1 and VPAC2 receptors. Hoechst was used to stain nuclei as blue.

4.3. Cholinergic-stimulated fluid secretion in isolated LG ducts

To investigate the role of CFTR in cholinergic-evoked ductal fluid secretion, the responses to muscarinic agonist carbachol were examined in WT and KO LG ducts both in HEPES and HCO_3^-/CO_2-buffered solution. Duct segments were isolated from 14 to 24-week-old mice. Rapid secretion could be observed in the first 4-5 minutes of carbachol stimulation

(100 μM) followed by a slower phase in HEPES buffered solution (secretory rates in the first 10 minutes of stimulation were: 134±5 pl/min/mm^2 in WT ducts, and 133±6 pl/min/mm^2 in KO ducts). Carbachol-evoked fluid secretory rates observed in WT and in KO ducts did not differ significantly in HEPES-buffered solution.

Carbachol-evoked fluid secretion in WT and in KO ducts superfused with HCO_3^-/CO_2--buffered solution was then investigated. Similarly to the results obtained in HEPES buffer a rapid secretory effect could be detected in the first 4-5 min both in WT and in KO ducts followed by slower secretion (secretory rates in the first 10 minutes of stimulation were: 133±6 pl/min/mm^2; in WT ducts; and 130±5 pl/min/mm^2 in KO ducts). Carbachol-evoked fluid secretion observed in WT and in KO ducts did not differ significantly in HCO_3^-/CO_2-buffered solution.

Briefly, carbachol stimulated fluid secretion in a similar manner both in WT and KO ducts and both in HEPES and HCO_3^-/CO_2-buffered solutions. There was not significant difference observed in secretory rates either between WT and KO ducts or between different buffers. Figure 4 and 5 demonstrate the carbachol-induced luminal volume changes in WT and KO ducts observed in HCO_3^-/CO_2-buffered solution.

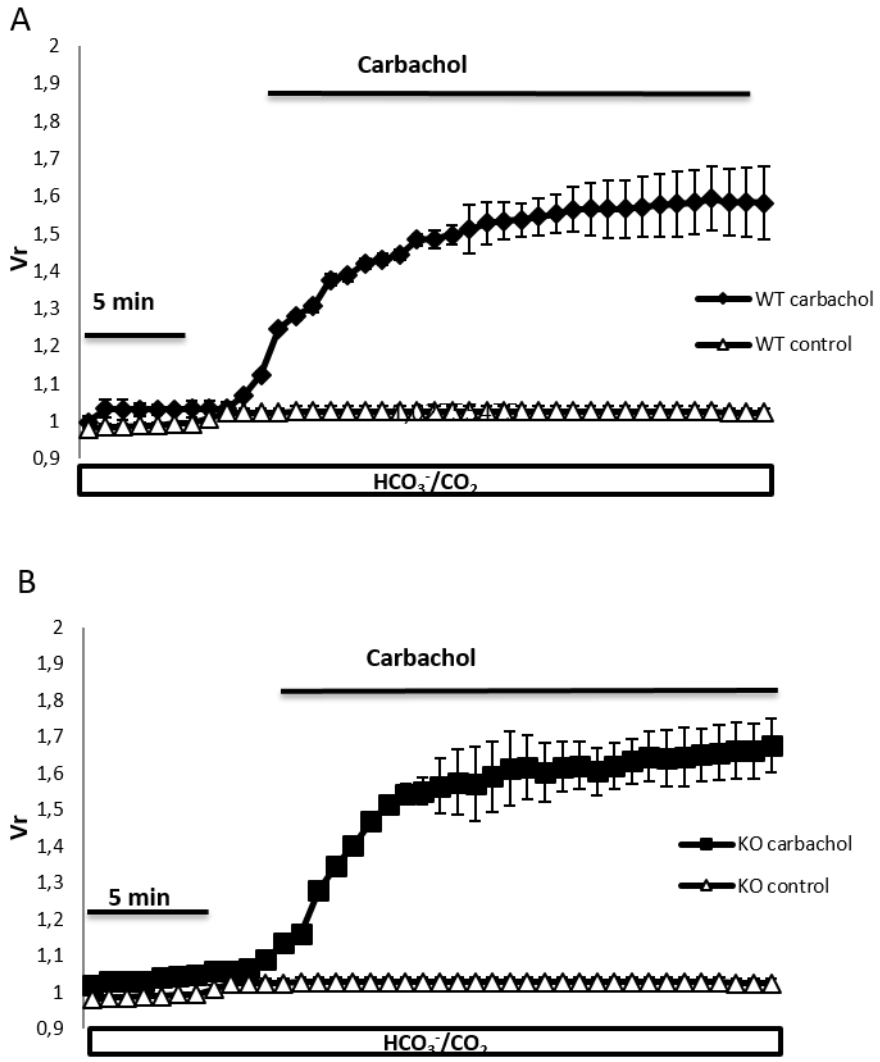

Figure 4: Effect of carbachol on ductal fluid secretion in LG ducts isolated from WT and CFTR KO mice. (A) WT ducts were exposed either to 100 μM carbachol (filled rhombus) or to no agonist (empty triangle). (B) KO ducts were exposed either to 100 μM carbachol (filled square) or to no agonist (empty triangle). Changes in relative lumial volume (Vr) are presented. Data were collected from 6 ducts isolated from 3 different animals in each series and are presented as means ±SEM.

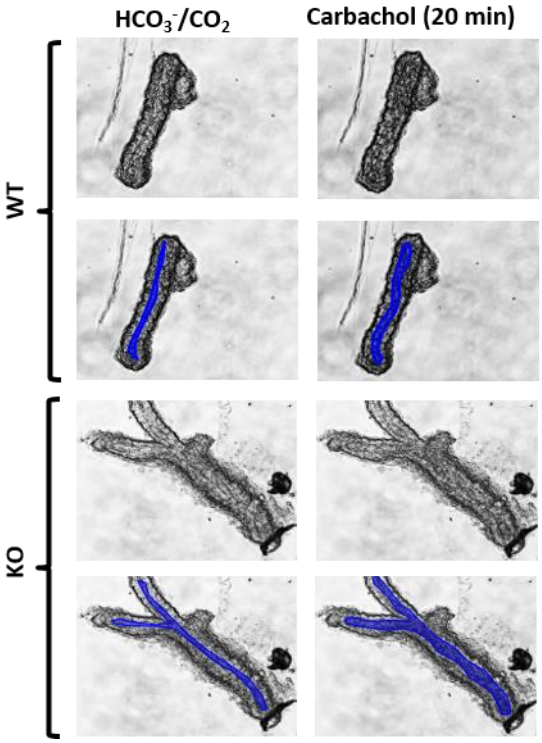

Figure 5: Demonstrative photo series of secreting isolated LG duct segments in response to carbachol stimulation. The luminal spaces of the native images (first and third rows) are marked with blue color (second and forth rows).

4.4. VIP-induced fluid secretion in isolated LG ducts

Effect of VIP (100 nM) on ductal fluid secretion was investigated on both WT and CFTR KO mouse LG ducts. These experiments were performed exclusively in HCO_3^-/CO_2-buffered solutions. Motives of solely HCO_3^-/CO_2 buffered experiments were partly the identical results obtained in different (HEPES and HCO_3^-/CO_2-) buffered solution in our previous experiments performed on different species. These results are displayed in the previous section and in our earlier publications. Furthermore, our VIP experiments were restricted to the HCO_3^-/CO_2 buffered solutions because of the difficulties observed during our VIP-stimulated fluid secretion experiments. In these experiments remarkable portion of isolated ducts missed to react to the applied agent. These findings are in accordance with our results in VPAC1 immunofluorescence studies where the expression of the receptor protein showed a mosaic pattern and the fluctuation of the presence of VPAC1 predicted an excessively altering response of the different duct segments to VIP stimulation. Obviously, all

data displayed in this section were obtained from the reacting (ie. responding with a swelling reaction) ducts.

VIP stimulation resulted in a robust and continuous fluid secretory response in isolated LG duct segments originated from WT mice (secretory rates in the first 10 minutes of stimulation were: 213.1±37.3 pl/min/mm^2, n=7). In contrast, CFTR KO ducts exhibited only a very weak pulse-like secretion in the first 5 minutes of stimulation (54.5±18.4 pl/min/mm^2, n=6), followed by a plateau (Figure 6). VIP-induced luminal volume changes in WT and KO ducts observed during videomicroscopic experiments demonstrated in Figure 7.

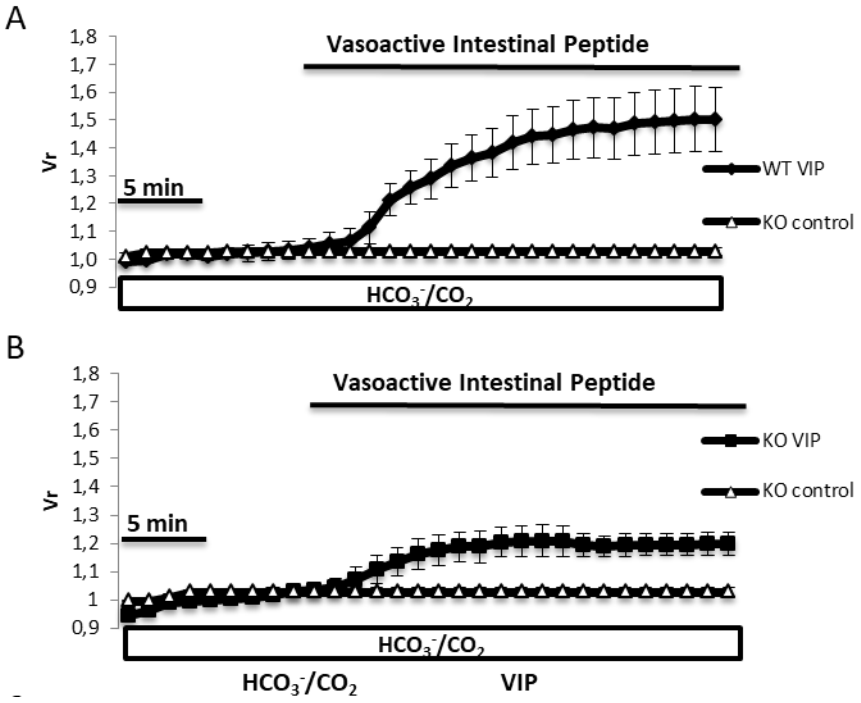

Figure 6: Effect of VIP stimulation on ductal fluid secretion in isolated LG ducts originated from WT and CFTR KO mice. (A) WT ducts were exposed either to 100 nM VIP (filled rhombus) or to no agonist (empty triangle). (B) CFTR KO ducts were exposed either to 100 nM VIP (filled square) or to no agonist (empty triangle). Changes in relative lumial volume (Vr) are presented. Data were obtained from 6 ducts isolated from 3 different animals in each series and are presented as means ±SEM.

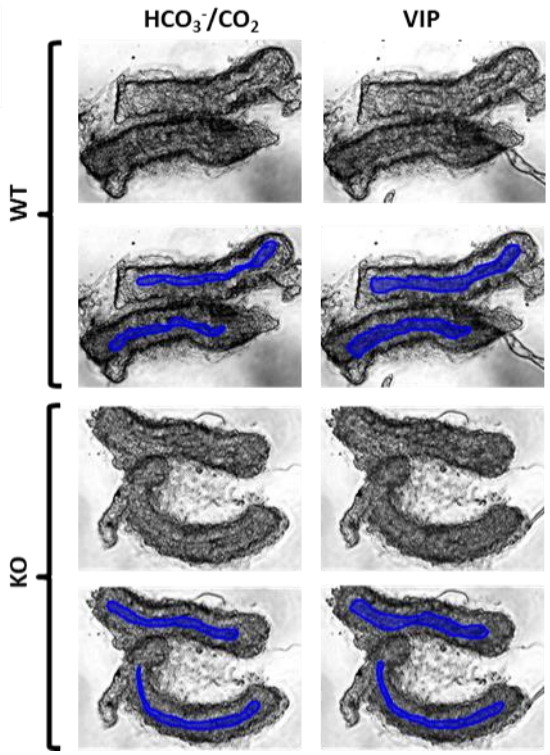

Figure 7: Demonstrative photo series of secreting isolated LG duct segments in response to VIP stimulation. The luminal spaces of the native images (first and third rows) are marked with blue color (second and forth rows).

4.5. Carbachol and VIP-induced Ca^{2+} signaling of isolated LG ducts

To investigate the effect of carbachol and the potential difference in $[Ca^{2+}]_i$ between WT and KO ducts, carbachol-evoked elevation of $[Ca^{2+}]_i$ was measured in both groups of isolated ducts. $[Ca^{2+}]_i$ was elevated by carbachol in a dose dependent manner both in WT ($F_{max(380/340)}$: 1 μM: 1.19±0.01; 10 μM: 1.67±0.05; 100 μM: 1.76±0.05) and in KO duct cells ($F_{max(380/340)}$: 1 μM: 1.15±0.02; 10 μM: 1.48±0.03; 100 μM: 1.83±0.05). Concentrations of carbachol over 100 μM proved to be citotoxic and therefore were excluded from our further experiments. No significant differences between WT and KO ducts were observed in these experiments (Figure 8).

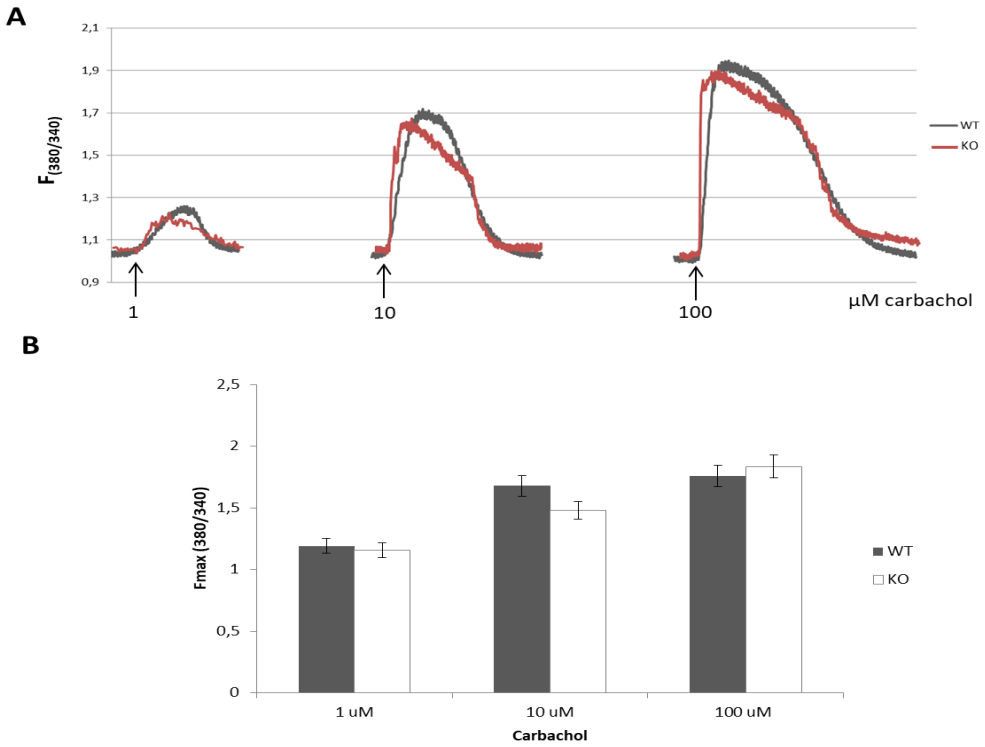

Figure 8: Effects of carbachol on $[Ca^{2+}]_i$ in LG duct cells from WT and KO mice. (A) Representative recordings of the microfluorescence experiments. (B) Carbachol dose-dependently elevated the $[Ca^{2+}]_i$, although no significant differences were found in the responses between ducts from WT and KO animals. $F_{380/340}$: 380/340 nm fluorescence emission ratio; $F_{max(380/340)}$: maximum value of the 380/340 nm fluorescence emission ratio.

Intracellular Ca^{2+} homeostasis underlying VIP stimulation was measured both in WT and in CFTR KO duct segments (Figure 9). Concentration of VIP was 100 nM in these experiments. This value was based on data from the literature and on our preliminary experiments where application of higher concentrations of VIP (200 and 500 nM) did not result in greater effects compared to the 100 nM concentration. VIP stimulation (100 nM) resulted in a small, but statistically significant increase in $[Ca^{2+}]_i$ both in WT (11.6±0.7%, p=0.001) and in CFTR KO ducts (11.1±0.5%, p=0.002). Cholinergic agonist carbachol (100 mM) was used as positive control in these experiments.

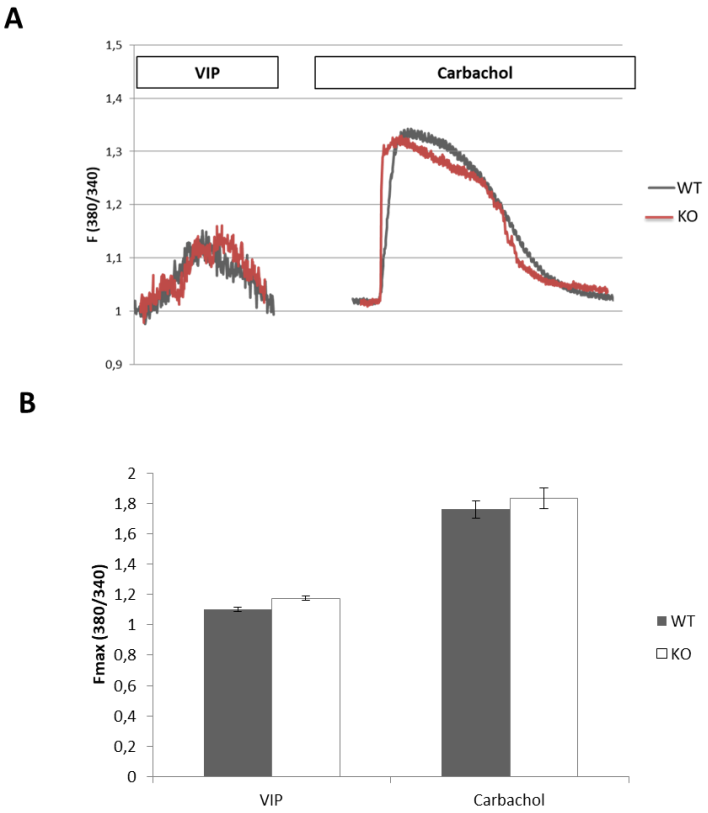

Figure 9: Effects of VIP and carbachol on $[Ca^{2+}]_i$ in LG duct cells from WT and KO mice. A) Representative recordings of the microfluorescence experiments: effects of VIP (100 nM) on $[Ca^{2+}]_i$ in LG duct cells from WT and KO mice (A, left curve). Carbachol (100 µM) was used for comparison - as a positive control - in these experiments (A, right curve). B) Maximum values of the 380/340 nm fluorescence emission ratios. $F_{380/340}$: 380/340 nm fluorescence emission ratio; $F_{max(380/340)}$: maximum value of the 380/340 nm fluorescence emission ratio.

5. DISCUSSION

Dry eye disease is an increasing health care problem in the industrialized countries affecting millions of people worldwide [32]. It has a deep impact on the patients'quality of life and induces a permanently increasing health care problem. Despite its growing economic effects, treatment options of the disease are limited. The management of the disease is a complex process but most of the available treatments focus on the alleviation of ocular symptoms, without targeting its underlying cause. Presently substitution of tear fluid with arteficial tear drops and – in severe cases – anti-inflammatory treatment of the ocular surface are the main but mostly insufficient interventions [33-35]. Appropriate amount of balanced electrolyte, protein and mucin composition of fluid secreted by the LG is fundamental for maintaining preocular tear film volume and integrity [1, 36]. Our understanding of the physiological and pathological mechanisms of LG secretion is limited, despite its critical importance in developing new treatment strategies. More detailed understanding of LG function is therefore essential in order to develop novel pharmacological approaches in the treatment of dry eye disease [7]. Unfortunately, duct cells have been understudied for many years compared to the widely investigated acinar cells. In the last decade, however, gene expression studies suggested the secretory role of LG duct epithelial cells, since greater expression of wide range of transmembrane transporters could be demonstrated in the duct cells compared to acinar cells [25, 37-41]. Although these results were important steps toward the clarification of duct cell function, they were unable to provide direct functional results. Our laboratory developed the first experimental model suitable for the investigation of lacrimal duct function, which opened a new way in lacrimal duct research. Our efforts are directed toward the clarification of the role of LG ducts in the secretory process of the gland using this isolated duct model [11,12] These viable duct segments are appropriate models not only for the investigation of the function of transmembrane transporters, but also for the investigation of the regulation of secretory machinery. Although secretory process of duct epithelium may play an important role in tear production, our knowledge about the regulation of LG duct function is rather limited. LG duct secretion is mediated by both parasympathetic and sympathetic systems [5,42,43]. The anatomically and functionally predominant parasympathetic nerves can be subdivided into two different branches based on the secreted neurotransmitters. Cholinergic nerve endings release the cholinergic agonist acetylcholine, while VIP-ergic nerve terminals produce VIP. Both neurotransmitters have

major effects on LG secretion [44]. The available experimental evidences about the role of the paraysmpathetic system in LG fluid secretion are solely from intact LGs or acini. We investigated the direct effect of the cholinergic and VIP-ergic stimuli on isolated LG duct segments, and explored the relationship between the CFTR chloride channel and the parasympathetic regulatory system. Transgenic mouse models carrying genetic defects in CFTR made it possible to set up experiments for investigating its role in fluid secretion and to shed light on the potential morphological alterations caused by the missing CFTR protein.

To assess the potential morphologic differences between LGs from CFTR KO and WT mice, histological examinations were performed on freshly dissected LGs. H&E staining revealed no obvious structural changes in CFTR KO LG tissues including ducts as compared to their age-matched WT counterparts. These results demonstrated that functional failure may present before morphological alterations during the course of disease progression. However, investigation of the morphological alterations in later stages of the disease in CFTR KO mice has strong limitations as shorter life expectancies of CFTR KO mice. Further studies are needed in order to clarify potential alterations in LG morphology later in life. In a case report of a CF patient, Alghadyan and colleagues observed increased number and size of vacuoles and a definite decrease in the number of the acini. They supposed that thickened mucus can occlude small ducts within the LG resulting in the degeneration of the acini and the appearance of vacuoles [45].

Immunofluorescence was used to confirm the presence and localization of CFTR, VPAC1 and VPAC2 proteins of mouse LG duct cells. Previous reports demonstrated the presence of CFTR mRNA and protein both in acinar and duct cells in rat and rabbit [9, 25, 39]. As demonstrated in Figure 2, we could observe intense CFTR staining most characteristically in the apical membranes of LG duct cells from WT animals. Some substantially weaker diffuse staining was also found in acinar cells, mostly within the cytoplasm. Although the appearance of CFTR protein is undoubted in acinar cells of mouse LG, our immunostaining results pointed its predominant presence in duct cells. These results suggest the important and duct-specific function of CFTR in LG similarly to its role in pancreatic ducts [46,47]. According to our expectations CFTR protein was not detectable in LGs of CFTR KO mice.

Presence and localization of VPAC1 and VPAC2 receptors was also investigated in LGs of both WT and CFTR KO mice. A previous report by Hodges et al. showed the presence of these receptors by immunostaining on the basolateral surface of both acinar and duct cells in rat [15]. An apparent difference was revealed in the distribution of VPAC1 and VPAC2

receptors in mouse LG in our study. Presence of VPAC1 was proved predominantly in ducts by immunoreactivity. Beside the characteristically ductal localization of VPAC1 receptors, a mosaic pattern in the expression of the receptor proteins was also revealed. Intensity of immunofluorescence varied excessively in the analyzed duct segments from the intense staining to the almost complete lack of demonstrability. VPAC2 showed a more homogeneous distribution in LG tissue: these receptors were traceable in both acinar and duct cells. Both VPAC1 and VPAC2 were observed most prominently on the basolateral membrane of mouse LG cells. Lack of CFTR did not influence the expression of VPAC1 and VPAC2 proteins: no difference was detected between the immunoreactivity of WT and CFTR KO LG tissues.

To explore the fluid secretory effect of parasympathetic neurotransmitters, videomicroscopic experiments were applied. Cholinergic agonist carbachol (100 μM) caused a biphasic fluid secretory response consisting of a rapid pulse-like secretion in the first 5 min, followed by a plateau. Similar secretory rates and patterns were observed in KO ducts, suggesting the independence of cholinergic activated secretory mechanisms from the presence of functionally active CFTR. VIP (100 nM) stimulation caused a strong and continuous fluid secretion in ducts from WT mice. In contrast, as a result of VIP stimulation, CFTR KO ducts exhibited only a weak pulse-like secretion in the first 5 min, followed by a plateau. The observed reduction in response to VIP stimulation in CFTR KO ducts may be explained by the lack of CFTR rather than changes of VPAC1 and VPAC2 since no difference was detected in the densitiy of VIP receptors between WT and CFTR KO ducts in our immunofluorescence studies. Role of CFTR can be explained by the following chain of effects: stimulation of VIP receptors increases the intracellular cAMP levels via adenylyl-cyclase then cAMP - as a potent activator - increases the activity of CFTR. Therefore, this transporter seems to be the determining component of the robust fluid secretion evoked by VIP in WT ducts. The weak secretory response observed in CFTR KO ducts during VIP stimulation seems to confirm the described mechanism.

Ca^{2+} homeostasis underlying parasympathetic stimulation and the potential role of CFTR protein was also investigated. The effect of carbachol and VIP stimuli on the cytosolic Ca^{2+} signaling was measured by microfluorometry. Carbachol induced a dose-dependent elevation of $[Ca^{2+}]_i$ in both WT and KO duct cells. The carbachol-evoked response of cytosolic Ca^{2+} level changes in WT and CFTR KO ducts did not differ significantly. The unchanged carbachol-evoked elevation of $[Ca^{2+}]_i$ in parallel with the unchanged carbachol-evoked secretory response in CFTR KO duct cells suggests the determining or exclusive role

of Ca^{2+} signaling in cholinergic stimulation and excludes the considerable function of CFTR in this pathway.

VIP also acts not only through the adenylyl cyclase-cAMP system but – in a smaller extent – it also elevated $[Ca^{2+}]_i$. VIP-evoked elevations of $[Ca^{2+}]_i$ were also independent from the presence of CFTR and did not differ in WT and CFTR KO LG ducts in a significant manner. However, elevations of $[Ca^{2+}]_i$ had a much smaller extent in case of VIP stimulation compared to the carbachol effect. Our findings in immunostaining studies and in fluid secretion together with $[Ca^{2+}]_i$ experiments suggests two, partially independent parasympathetic regulatory pathways. Briefly, carbachol stimulation acts solely through elevation of $[Ca^{2+}]_i$ and it does not involve adenylyl cyclase-cAMP route. Consequently, CFTR is not involved in carbachol stimulated fluid secretion as it is activated by cAMP. For VIP stimuli $[Ca^{2+}]_i$ was slightly elevated without significant difference between the values measured in WT and CFTR KO ducts. However, secretory response of LG ducts showed a great significant difference in WT and CFTR KO ducts: rate of fluid secretion of CFTR KO ducts was far below the value obtained in WT ducts. These data prove the determining role of adenylyl cyclase-cAMP-CFTR route in VIP-stimulated fluid secretion of LG ducts. Results of our VIP experiments are in accordance with previous observations that VIP acts predominantly through elevation of cytosolic cAMP level, the minority of its action thougt to be mediated by Ca^{2+} signaling [48-50]. Lack of functionally active CFTR seen in CFTR KO mice influences VIP-evoked secretory response of LG ducts and thus can modify the total parasympathetic-evoked secretory answer of the LGs. CFTR could influence LG secretion through the modification of ductal secretion and therefore defects in CFTR may significantly compromise Cl^- and water secretion from LG ducts.

6. SUMMARY

In conclusion, our results presented here provide new proof of the secretory role of LG ducts beside their piping function. We demonstrated the functional presence of CFTR and VIP receptors in LG duct cells. Strong predominance of CFTR protein on the apical, VPAC1 and VPAC2 on the basolateral surface of the duct cells was observed. Fluid secretory experiments provided direct functional evidence of the importance of parasympathetic regulation in LG ducts. The observed carbachol- and VIP-induced significant fluid secretion suggests the importance of these secretagouges on the fluid secretion of the duct system.

We detected the elevation $[Ca^{2+}]_i$ for the stimuli of carbachol an VIP, and the preservation of the Ca^{2+} signaling pathway in CFTR KO mice. These results reveal new insight into the role of VIP in LG function and confirm the connection between CFTR and VIP regulatory pathways. Further studies are needed to clarify whether modification of CFTR or VIP function may serve as a potential target to stimulate LG secretion and therefore can be an option in treating aqueous deficient dry eye.

Conclusions of the studies on LG ducts presented in the thesis are:

1. **CFTR is dominantly expressed on the apical membrane of the LG duct cells compared to acinar cells in mice**
2. **VPAC1 receptors are expressed predominantly in the duct cells, while VPAC2 receptors are expressed in both duct and acinar cells in mice LG. VPAC1 and VPAC2 receptors are located on the basolateral membranes.**
3. **For the first time in LG research, CFTR KO mice were used to study the role of parasympathetic regulation in LG duct function and to study the role of CFTR in the parasympathetic secretory machinery**
4. **Using our isolated duct segment model developed earlier, fluid secretion of LG ducts from WT and CFTR KO mice was investigated by videomicroscopic methods. Significant fluid secretion was observed as a result of carbachol and VIP stimulation.**
5. **The significant secretory response of LG ducts from KO mice for carbachol stimuli showed the independence of cholinergic activated secretory mechanisms from the presence of functionally active CFTR.**
6. **Role of CFTR in the VIP-induced secretory process found to be decisive as only small VIP-induced fluid secretion was detected in the absence of CFTR protein.**

7. **Similar elevations of $[Ca^{2+}]_i$ levels in WT and KO ducts - both in case of carbachol and VIP stimuli - demonstrated the independence of $[Ca^{2+}]_i$ homeostasis from the functionally active CFTR.**

7. ACKNOWLEDGEMENTS

I would like to thank all of the people who have helped and inspired me during my PhD studies.

First of all I express my gratitude and appreciation to **Dr. Edit Tóth-Molnár**, the head of the the Department of Ophthalmology, who always helped and guided me during my PhD studies. Her knowledge, attitude and advices inspired and helped me to complete this work.

I am grateful to **Prof. Dr. András Varró**, the former head of Department of Pharmacology and Pharmacotherapy who gave me opportunity to work at his Department.

I also would like to say thank you for **Prof. Dr. Péter Hegyi** and **Prof. Dr. Zoltán Rakonczay Jr**. for the opportunity to do my research in their laboratory.

In addition, I would like to thank my colleagues and friends, **Júlia Fanczal, Dr. Máté Katona, Dr. Eszter Vizvári, Dóra Szarka** and **all members of the Pancreas Research Group** for all the help, entertainment and care they provided.

I have to say a special thanks to **Farkas Borics-Berczeli and Dr. Attila Borics** for their love and patience during my PhD studies.

Last, but not least I owe warm thanks to **my mother Ágnes Kovács and my brother Ákos Berczeli and my whole family** for all their love, support and encouragement.

I dedicate this thesis to them!

8. REFERENCES

1. Conrady CD, Joos ZP, Patel BC. Review. The Lacrimal Gland and Its Role in Dry Eye. **J Ophthalmol** 2016; 2016:7542929 doi.
2. Craig JP, Nichols KK, Akpek EK et al. TFOS DEWS II Definition and Classification Report. **Ocul Surf** 2017; 15: 276-283.
3. Hodges RR, Dartt DA. Tear film mucins: front line defenders of the ocular surface; comparison with airway and gastrointestinal tract mucins. **Exp Eye Res** 2013; 117:62-78.
4. Willcox MDP, Argüeso P, Georgiev GA et al. TFOS DEWS II Tear Film Report. **Ocul Surf** 2017; 15: 366-403.
5. Dartt DA. Neural regulation of lacrimal gland secretory processes: relevance in dry eye diseases. **Prog Retin Eye Res** 2009; 28:155-77.
6. Gilbard JP, Dartt DA, Rood RP et al. Increased tear secretion in pancreatic cholera: a newly recognized symptom in an experiment of nature. **Am J Med** 1988; 85:552-4.
7. Alexander JH, van Lennep EW, Young JA. Water and electrolyte secretion by the exorbital lacrimal gland of the rat studied by micropuncture and catheterization techniques. **Pflugers Arch** 1972;337 299-309.
8. Dartt DA, Moller M, Poulsen JH. Lacrimal gland electrolyte and water secretion in the rabbit: localization and role of (Na^+-K^+)-activated ATPase. **J Physiol** 1981; 321: 557-69.
9. Ubels JL, Hoffman HM, Srikanth S, Resau JH, Webb CP. Gene expression in rat lacrimal gland duct cells collected using laser capture microdissection: evidence for Kþ secretion by the duct cells. **Invest Ophthalmol Vis Sci** 2006; 47:1876-1885.
10. Tóth-Molnár E, Venglovecz V, Ozsvári B, et al. New experimental method to study acid/base transporters and their regulation in lacrimal gland ductal epithelia. **Invest Ophthalmol Vis Sci** 2007; 48:3746-3755.
11. Katona M, Vizvári E, Németh L, et al. Experimental evidence of fluid secretion of lacrimal gland duct epithelium. **Invest Ophthalmol Vis Sci** 2014;55:4360-4367.
12. Fernández-Salazar MP, Pascua P, Calvo JJ, et al. Basolateral anion transport mechanisms underlying fluid secretion by mouse, rat and guinea-pig pancreatic ducts. **J Physiol** 2004; 556.2:415-428.
13. Said SI, Mutt V. A peptide fraction from lung tissue with prolonged peripheral vasodilator activity. **Scand J Clin Lab Invest Suppl**1969; 107: 51-6.

14. Laburthe M, Couvineau A, Tan V. Class II G protein-coupled receptors for VIP and PACAP: structure, models of activation and pharmacology. **Peptides** 2007; 28: 1631-9.
15. Hodges RR, Zoukhri D, Sergheraert C, Zieske JD, Dartt DA. Identification of vasoactive intestinal peptide receptor subtypes in the lacrimal gland and their signal-transducing components. **Invest Ophthalmol Vis Sci** 1997; 38: 610-9.
16. Hong JH, Park S, Shcheynikov N, Muallem S. Mechanism and synergism in epithelial fluid and electrolyte secretion. **Pflugers Arch**2014; 466: 1487-99.
17. Lee MG, Ohana E, Park HW, Yang D, Muallem S. Molecular mechanism of pancreatic and salivary gland fluid and HCO_3 secretion. **Physiol Rev** 2012; 92:39-74.
18. Quinton PM. Physiological basis of cystic fibrosis: a historical perspective. **Physiol Rev** 1999; 79:S3-S22.
19. Reddy MM, Quinton PM. PKA mediates constitutive activation of CFTR in human sweat duct. **J Membr Biol** 2009; 231:65-78.
20. Roussa E. Channels and transporters in salivary glands. **Cell Tissue Res** 2011; 343: 263-87.
21. Steward MC, Ishiguro H. Molecular and cellular regulation of pancreatic duct cell function. **Curr Opin Gastroenterol** 2009; 25:447-53.
22. Castagna I, Roszkowska AM, Fam`a F, Sinicropi S, Ferreri G. The eye in cystic fibrosis. **Eur J Ophthalmol** 2001; 11:9–14.
23. Mrugacz M, Kaczmarski M, Bakunowicz-Lazarczyk A, Zelazowska B, Wysocka J, Minarowska A. IL8 and IFN-gamma in tear fluid of patients with cystic fibrosis. **J Interferon Cytokine Res** 2006; 26:71–75.
24. Sheppard JD, Orenstein DM, Chao CC, Butala S, Kowalski RP. The ocular surface in cystic fibrosis. **Ophthalmology** 1989; 96:1624–130.
25. Ding C, Parsa L, Nandoskar P, Zhao P, Wu K, Wang Y. Duct system of the rabbit lacrimal gland: structural characteristics and role in lacrimal secretion. **Invest Ophthalmol Vis Sci** 2010; 51:2960–2967.
26. Lu M, Ding C. CFTR-mediated Cl^- transport in the acinar and duct cells of rabbit lacrimal gland. **Curr Eye Res** 2012; 37: 671-7.
27. Frizzell RA, Hanrahan JW. Physiology of epithelial chloride and fluid secretion. **Cold Spring Harb Perspect Med** 2012; 2: a009563.
28. Hwang TC, Kirk KL The CFTR ion channel: gating, regulation, and anion permeation. **Cold Spring Harb Perspect Med** 2013; 3: a009498.

29. Keiser NW, Engelhardt JF. New animal models of cystic fibrosis: what are they teaching us? **Curr Opin Pulm Med** 2011;17:478–483.
30. Ratcliff R, Evans M J, Cuthbert AW, MacVinish LJ, Foster D, Anderson JR, Colledge WH: Production of a severe cystic fibrosis mutation in mice by gene targeting. **Nat Genet** 1993; 4:35–41.
31. Seidler U, Singh A, Chen M, et al. Knockout mouse models for intestinal electrolyte transporters and regulatory PDZ adaptors: new insights into cystic fibrosis, secretory diarrhoea and fructose-induced hypertension. **Exp Physiol** 2009; 94:175– 179.
32. Stapleton F, Alves M, Bunya VY. TFOS DEWS II Epidemiology Report. **Ocul Surf** 2017; 15: 334-365.
33. Jones L, Downie LE, Korb D. TFOS DEWS II Management and Therapy Report. **Ocul Surf** 2017; 15:575-628.
34. Milner MS, Beckman KA, Luchs JI. Dysfunctional tear syndrome: dry eye disease and associated tear film disorders - new strategies for diagnosis and treatment. Curr Opin **Ophthalmol** 2017; 27:3-47.
35. The definition and classification of dry eye disease: report of the Definition and Classification Subcommittee of the International Dry Eye WorkShop (2007). **Ocul Surf** 2007. 5(2): p. 75-92.
36. Walcott B. The Lacrimal Gland and Its Veil of Tears. **News Physiol Sci** 1998;13:97-103.
37. Ding C, Lu M, and Huang J. Changes of the ocular surface and aquaporins in the lacrimal glands of rabbits during pregnancy. **Mol Vis** 2011; 17:2847-55.
38. Ding C, Nandoskar P, Lu M. Changes of aquaporins in the lacrimal glands of a rabbit model of Sjogren's syndrome. **Curr Eye Res** 2011; 36:571-8.
39. Nandoskar P, Wang Y, Wei R, Liu Y. Changes of chloride channels in the lacrimal glands of a rabbit model of Sjogren syndrome. **Cornea** 2012; 31:273-9.
40. Thomson-Vest N, Shimizu Y, Hunne B, Furness JB. The distribution of calcium-activated, intermediate conductance potassium (IK) channels in epithelial cells. **J Anat** 2006; 208: 219-29. doi: 10.1111/j.1469-7580.2006.00515.x.
41. Walcott B, Birzgalis A, Moore LC, Brink PR. Fluid secretion and the Na+-K+-2Cl– cotransporter in mouse exorbital lacrimal gland. **Am J Physiol Cell Physiol** 2005; 289: C860–C867. doi:10.1152/ajpcell.00526.2004.
42. Ding C, Walcott B, Keyser KT. Sympathetic neural control of the mouse lacrimal gland. **Invest Ophthalmol Vis Sci** 2003; 44(4):1513-20.

43. Ding C, Walcott B, Keyser KT. Alpha 1- and beta 1- adrenergic modulation of lacrimal gland function in the mouse. **Invest Ophthalmol Vis Sci** 2007; 48:1504-10. doi: 10.1167/iovs.05-1634.
44. Dartt DA. Signal transduction and control of lacrimal gland protein secretion: a review. **Curr Eye Res** 1989; 8:619-36.
45. Alghadyan A, Aljindan M, Alhumeidan A, Kazi G, McMhon R. The lacrimal glands in cystic fibrosis. **Saudi J Ophthalmol** 2013; 27:113–116.
46. Ishiguro H, Steward MC, Wilson RW, Case RM. Bicarbonate secretion in interlobular ducts from quinea-pig pancreas. **J Physiol** 1996; 495.1:179-191.
47. Ishiguro H, Yamamoto A, Nakakuki M, Yi L, Ishiguro M, Yamaguchi M et al. Physiology and pathophysiology of bicarbonate secretion by pancreatic duct epithelium. **Nagoya J Med Sci** 2012; 74:1-18.
48. Dérand R, Montoni A, Bulteau-Pignoux L. Activation of VPAC1 receptors by VIP and PACAP-27 in human bronchial epithelial cells induces CFTR-dependent chloride secretion. **Br J Pharmacol** 2004; 141:698-708.
49. Dickson L, Aramori I, McCulloch J. A systematic comparison of intracellular cyclic AMP and calcium signalling highlights complexities in human VPAC/PAC receptor pharmacology. **Neuropharmacology** 2006; 51:1086-98.
50. Xia M, Sreedharan SP, Goetzl EJ. Predominant expression of type II vasoactive intestinal peptide receptors by human T lymphoblastoma cells: transduction of both Ca^{2+} and cyclic AMP signals. **J Clin Immunol** 1996; 16:21-30.